

# Accepted Manuscript

Research paper

Synthesis and characterization of magnetically separable  $\text{Fe}_3\text{O}_4@ \text{AHBA}@\text{Ni}(0)$  [AHBA = 3-amino-4-hydroxybenzoic acid] nanocatalyst: applications for carbonyl hydrogenation and alcohol oxidation

Sanchari Dasgupta, Aratrika Chakraborty, Sourav Chatterjee, Tanmay Chattopadhyay

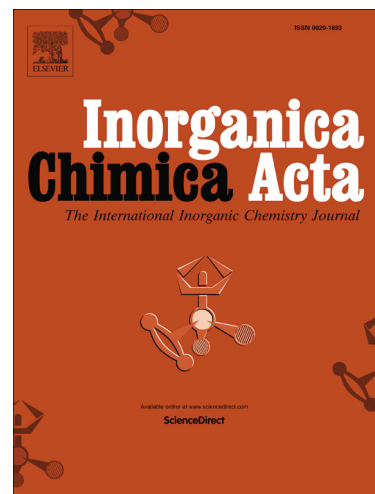
PII: S0020-1693(17)30281-5  
DOI: <https://doi.org/10.1016/j.ica.2018.01.009>  
Reference: ICA 18083

To appear in: *Inorganica Chimica Acta*

Received Date: 24 February 2017  
Revised Date: 5 January 2018  
Accepted Date: 8 January 2018

Please cite this article as: S. Dasgupta, A. Chakraborty, S. Chatterjee, T. Chattopadhyay, Synthesis and characterization of magnetically separable  $\text{Fe}_3\text{O}_4@ \text{AHBA}@\text{Ni}(0)$  [AHBA = 3-amino-4-hydroxybenzoic acid] nanocatalyst: applications for carbonyl hydrogenation and alcohol oxidation, *Inorganica Chimica Acta* (2018), doi: <https://doi.org/10.1016/j.ica.2018.01.009>

This is a PDF file of an unedited manuscript that has been accepted for publication. As a service to our customers we are providing this early version of the manuscript. The manuscript will undergo copyediting, typesetting, and review of the resulting proof before it is published in its final form. Please note that during the production process errors may be discovered which could affect the content, and all legal disclaimers that apply to the journal pertain.



**Synthesis and characterization of magnetically separable Fe<sub>3</sub>O<sub>4</sub>@AHBA@Ni(0) [AHBA = 3-amino-4-hydroxybenzoic acid] nanocatalyst: applications for carbonyl hydrogenation and alcohol oxidation**

**Sanchari Dasgupta,<sup>a</sup> Aratrika Chakraborty,<sup>a</sup> Sourav Chatterjee,<sup>b</sup> Tanmay Chattopadhyay<sup>\*,b</sup>**

<sup>a</sup>*Department of Chemistry, University of Calcutta, 92 A. P. C. Road, Kolkata-700009, India*

<sup>b</sup>*Department of Chemistry, Panchakot Mahavidyalaya, Sarbari, Purulia, 723121, India.*

*E-mail: tanmayc2003@gmail.com*

## **ABSTRACT**

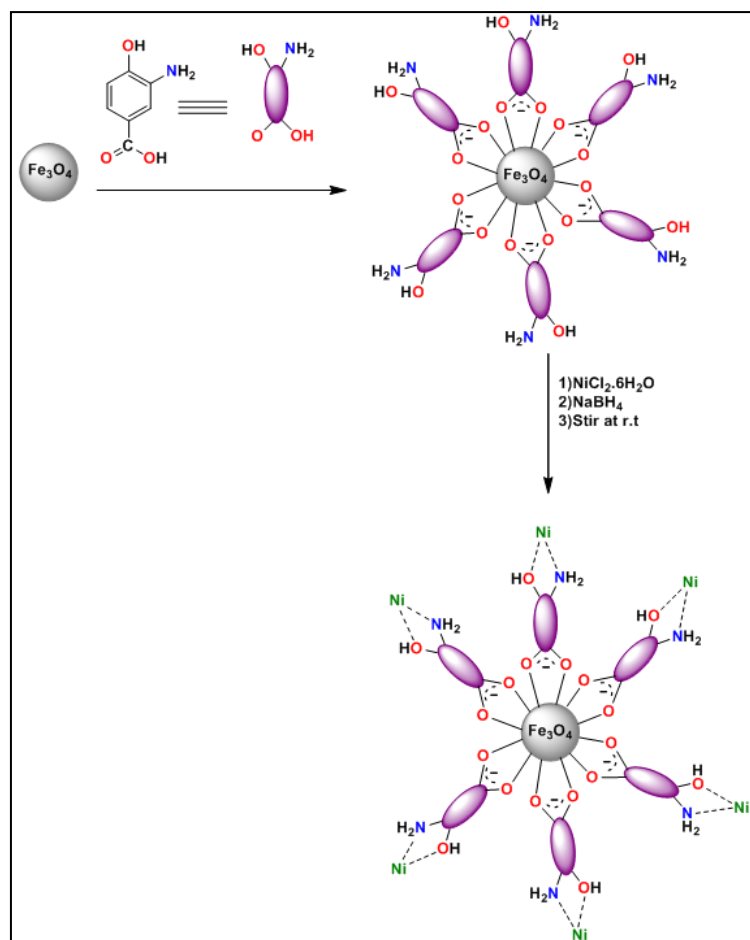
A simple, facile and convenient practical method has been developed for the preparation of a magnetically separable nanocatalyst, Fe<sub>3</sub>O<sub>4</sub>@AHBA@Ni(0) [AHBA = 3-amino-4-hydroxybenzoic acid]. The synthesized nanocatalyst was characterized by electron microscopy techniques (SEM, TEM with EDX), Power X-Ray Diffraction (PXRD), Fourier transform infrared spectroscopy (FT-IR) and solid state UV-Vis spectroscopy techniques. X-Ray photoelectron spectroscopy (XPS) study and time of flight secondary ion mass spectroscopy (TOF-SIMS) study unambiguously prove the presence of nickel(0) on the surface of Fe<sub>3</sub>O<sub>4</sub>. The surface area of prepared catalyst has been achieved 330 m<sup>2</sup> g<sup>-1</sup> from BET surface area analysis. This catalyst exhibits appreciable activity towards carbonyls reduction and alcohols oxidation by changing the reaction conditions. The salient feature of the present protocol is that the catalyst can be separated simply through an external magnetic field and recycled for several times without any significant deterioration in its activity. Moreover, ambient reaction conditions, easy workup process, extensive substrate scope and cost effectiveness are some of the other wonderful features of this procedure that make it cheap and sustainable.

**Key words:** Magnetic nanoparticles, Nickel(0), Catalysis, Recyclable, Oxidation, Reduction

## **1. Introduction**

The field of nanoparticles has invited appreciable success because they have tremendous potential to serve as catalysts owing to their active surface and interfacial atom effect, easy recovery and reusability.[1-4] But unsupported nanoparticles are often unstable, and agglomeration is frequently unavoidable during the reactions.[5] Thus, to overcome this

difficulty, nanoparticles have been immobilized on different solid supports.[6-12] But, again the separation of these catalysts from reaction medium is very difficult.[13] Therefore, surface modified magnetically separable super paramagnetic nanoparticles appear as a redeemer.[14-22] Considering the fact that the position of nickel lies just above palladium and platinum in the periodic table hence it can perform many of the same basic reactions as palladium or platinum. The oxidation and reduction of organic functionalities is extremely important in organic synthesis and has wide application in industry. In particular, very costly metal nanoparticles, such as Pd, Pt and Au etc. have been evaluated for their ability to catalyze these reactions.[23-24] Currently, nickel catalysed reactions is encountering a period of escalated interest.[25] Practically speaking, the cost of nickel is lower than noble metals. Again, as a first row transition metal, nickel has a small atomic radius, thus Ni-ligand bond lengths are often relatively short and strong.[26] Although the field of nickel catalysis has rapidly expanded over the last decade,[27-32] still there are many challenges that are yet to be conquered. Presently, we are deeply involved in the field of catalysis to find out new cost effective catalytic systems.[14,33-35] Here, we have reported a magnetically separable new nickel catalyst that is highly active for both alcohol oxidation and carbonyl reduction. To the best of our knowledge, this is the first example of such a catalyst that performs the two reactions by changing the conditions only. Moreover, the catalyst can be easily recovered by magnet and recycled several times without significant loss its activity. In this perspective a novel  $\text{Fe}_3\text{O}_4@\text{AHBA}@\text{Ni}(0)$  [AHBA=3-amino-4-hydroxybenzoic acid] catalyst has been synthesized (Scheme 1). Topark *et al* employed carboxylate group of piperidine-4-carboxylic acid to modify the surface of  $\text{Fe}_3\text{O}_4$  nanoparticles.[36] Here we have used AHBA for similar purpose and it acts as a connector between  $\text{Fe}_3\text{O}_4$  and Ni(0). Attachment of the carboxylate group of AHBA to  $\text{Fe}_3\text{O}_4$  nanoparticles and formation of five member chelate ring by its free amino and hydroxyl group with Ni(0) enhances the stability of our synthesized nanocatalyst. Moreover this newly synthesized catalyst is cost effective. Fortunately our prepared catalyst can work for two types of catalytic reaction: (i) carbonyl reduction, and (ii) alcohol oxidation.



**Scheme 1.** Schematic diagram of preparation of  $\text{Fe}_3\text{O}_4@AHBA@Ni(0)$  catalyst.

## 2. Experimental details

### 2.1. Materials and methods.

All chemicals were obtained from commercial sources and used as received. Solvents were dried according to standard procedure and distilled prior to use.  $\text{FeSO}_4 \cdot 7\text{H}_2\text{O}$ ,  $\text{FeCl}_3 \cdot 6\text{H}_2\text{O}$ ,  $\text{NiCl}_2 \cdot 6\text{H}_2\text{O}$ , sodium borohydride, hydrogen peroxide, alcohols and aldehydes were purchased from merck and 3-amino-4-hydroxybenzoic acid,  $\text{CDCl}_3$  was purchased from sigma Aldrich. Infrared spectra ( $2000\text{--}500\text{ cm}^{-1}$ ) were recorded at  $27^\circ\text{C}$  using a Perkin-Elmer RXI FT-IR spectrophotometer with KBr pellets. Electronic spectra ( $800\text{--}200\text{ nm}$ ) were obtained at  $27^\circ\text{C}$  using a Shimadzu UV-3101PC with methanol as solvent and reference. Thermal analyses (TG-DTA) were carried out on a Mettler Toledo (TGA/SDTA851) thermal analyzer in flowing dinitrogen (flow rate:  $30\text{ cm}^3\text{ min}^{-1}$ ). Scanning Electron Microscope (SEM) measurement was carried out with JEOL JSM-6700F field-emission microscope. X-ray powder diffraction (PXRD) was performed on a XPERT-PRO Diffractometer

monochromated Cu-K $\alpha$  radiation (40.0 kV, 30.0 mA) at room temperature. The spectra of the samples were recorded at room temperature in solid phase. The light irradiation dependent study was done after different irradiation times with a white light source compiled with a <420 nm cut off filter. A vibrating sample magnetometer (EV-9, Microsense, ADE) was utilized for obtaining the magnetization curves. Electrospray mass spectra have been recorded on a WATERS Xevo G2-S Q ToF mass spectrometer.

## 2.2. Synthesis of Fe<sub>3</sub>O<sub>4</sub> NPs.

Preparation of magnetically responsive Fe<sub>3</sub>O<sub>4</sub> NPs was prepared following the same procedure as reported earlier.[37]

## 2.3. Synthesis of Fe<sub>3</sub>O<sub>4</sub>@AHBA.

3 g of 3-amino-4-hydroxybenzoic acid (AHBA) was dissolved in 10 mL of ethanol. This solution was added to ethanolic suspension of 3 g of Fe<sub>3</sub>O<sub>4</sub> and was stirred for 24 h at room temperature. The product was then allowed to settle, collected by centrifugation and washed several times with ethanol. The products were air dried.

## 2.4. Synthesis of Fe<sub>3</sub>O<sub>4</sub>@AHBA@Ni(II).

Fe<sub>3</sub>O<sub>4</sub>@AHBA was dispersed in water and NiCl<sub>2</sub>.6H<sub>2</sub>O solution in water was added drop wise to get the 10 weight % of nickel. The reaction mixture was stirred for 24 h at room temperature. The product was allowed to settle and was washed several times with water and acetone and dried under vacuum at 60°C for 2 h.

## 2.5. Synthesis of Fe<sub>3</sub>O<sub>4</sub>@AHBA@Ni(0).

Fe<sub>3</sub>O<sub>4</sub>@AHBA was dispersed in water and NiCl<sub>2</sub>.6H<sub>2</sub>O solution in water was added drop wise to get the 10 weight % of nickel. After that 0.1 g of NaBH<sub>4</sub> was added portion wise. The reaction mixture was stirred for 24 h at room temperature. The product was allowed to settle and was washed several times with water and acetone and dried under vacuum at 60 °C for 2 h.

## 2.6. General procedure of reduction of aldehydes.

Aldehydes (1 mmol), KOH ( 2 mmol), catalyst 30 mg) were stirred in 3 mL of glycerol at room temperature for appropriate time. The progress of the reaction was monitored by TLC. The catalyst was separated magnetically and the product was extracted with ethyl acetate and

the organic layer was evaporated in vacuum. The crude product thus obtained was purified by column chromatography on silica gel using n-hexane and ethyl acetate as eluent.

### 2.7. General procedure of oxidation of alcohols.

The alcohol (1 mmol), catalyst (20 mg),  $\text{PhI}(\text{OAc})_2$  (403 mg, 1.25 mmol) and  $\text{MgSO}_4$  (about 300 mg) were stirred in ethylenedichloride (EDC, 25 mL) at room temperature until the reaction was complete. The progress of the reaction was monitored by TLC. The reaction mixture was filtered through sintered funnel and residue was washed with EDC. Then the EDC layer was washed with water and dried over anhydrous  $\text{MgSO}_4$ . The solvent was removed using rotary evaporator at room temperature under reduced pressure. The crude product was purified by column chromatography over silica gel using ethyl acetate–petroleum ether as eluent.

## 3. Results and discussions.

### 3.1. Characterization of $\text{Fe}_3\text{O}_4@AHBA@Ni(0)$ .

Magnetically active  $\text{Fe}_3\text{O}_4$  nanoparticles (here after  $\text{Fe}_3\text{O}_4$  NPs) were prepared following the same procedure as reported earlier.[14, 32–34]  $\text{Fe}_3\text{O}_4@AHBA$  was prepared by stirring of AHBA (3 gm) and  $\text{Fe}_3\text{O}_4$  NPs (3 gm) for 24 h in ethanolic medium.

Primarily the UV-Vis spectra was taken in solution phase for homogeneous catalyst to ensure the reduction of Ni(II)-AHBA complex to Ni(0)-AHBA. Before the reduction was performed the d-d band of Ni(II)-AHBA complex is observed at 761 nm which gradually vanishes upon addition of  $\text{NaBH}_4$ . The reduced Ni(0)-AHBA was then separated and FT-IR and Solid state UV-Vis spectra was recorded (Fig.1).

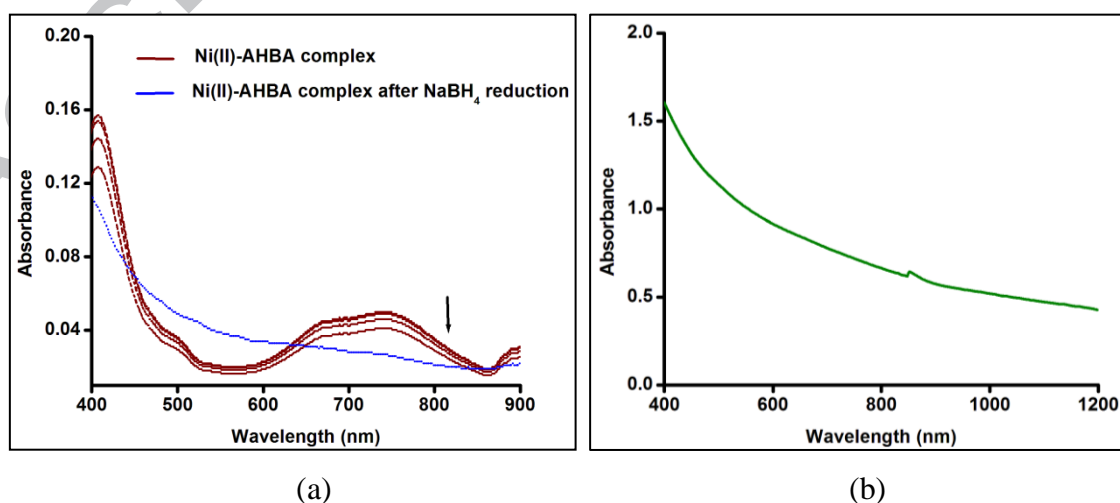


**Fig. 1.** (a) Reduction of d-d band of Ni(0) upon addition of  $\text{NaBH}_4$  and (b) Solid state UV-Vis Spectra of Ni(0)-AHBA complex

The Fourier transform infra-red (FT-IR) contains a band at  $1600\text{ cm}^{-1}$  which is a signature of C=O stretching of carboxylic acid group of AHBA moiety which is also present in case of Ni(0)-AHBA complex [14] and the bands at  $620$  and  $586\text{ cm}^{-1}$  are due to  $\text{Fe}_3\text{O}_4$  NPs which is signature of Fe-O vibration (Fig. S1). The characteristic band for NiO is not observed in FT-IR spectrum of  $\text{Fe}_3\text{O}_4@AHBA@Ni(0)$ . [38]

We did not observe of any characteristics bands of  $\text{Ni}^{2+}$  in the solid state UV-Vis spectrum of the  $\text{Fe}_3\text{O}_4@AHBA@Ni(0)$ . This result hints that Ni(0) present at the surface of  $\text{Fe}_3\text{O}_4@AHBA$  (Fig. S2).

Thermal stability of  $\text{Fe}_3\text{O}_4$ ,  $\text{Fe}_3\text{O}_4@AHBA$  and  $\text{Fe}_3\text{O}_4@AHBA@Ni(0)$  was studied by thermo gravimetric analysis (TGA). The thermo gram of the  $\text{Fe}_3\text{O}_4$  consist of about 6.5% loss of weight in the range of  $30-800\text{ }^\circ\text{C}$ . The TGA curve of  $\text{Fe}_3\text{O}_4@AHBA@Ni(0)$  demonstrates a weight loss about 19% from  $260$  to  $800\text{ }^\circ\text{C}$ , due to the decomposition of organic materials grafting to the  $\text{Fe}_3\text{O}_4$  surface (Fig. S3). This result confirms the successful grafting of AHBA and Ni(0) on the  $\text{Fe}_3\text{O}_4$  NPs.

The X-Ray photoelectron spectroscopy (XPS) study was carried out to determine the surface composition of the nanoparticle. Oxygen appears as most abundant element with percentage ratio 60.7 and the percentage of Ni present to the surface of catalyst is 7.6. The characteristic bands of nickel (Ni 2p) is depicted in Fig. 2. The peaks at  $854.3$  and  $871.9\text{ eV}$  are assigned to Ni(0)  $2p_{3/2}$  and Ni(0)  $2p_{1/2}$  and, respectively. Two lower intensity peaks at  $860.1$  and  $878.09\text{ eV}$  can be assigned to Ni(II)  $2p_{3/2}$  and Ni(II)  $2p_{1/2}$ , respectively which suggests that NiO was present as impurity in very low concentration. From the peak position it can be easily concluded that Nickel(0) is present at the surface of the catalyst. [39-43]

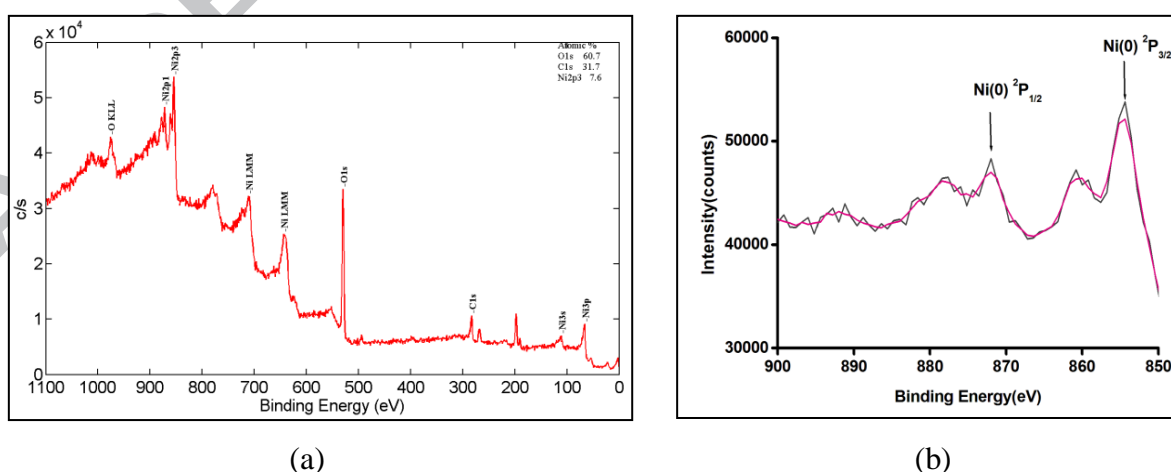


**Fig. 2.** X-ray photoelectron spectroscopy of  $\text{Fe}_3\text{O}_4@AHBA@Ni(0)$  (a) taken in full range and (b) characteristics band of Ni(0)

Oxidation of nickel(0) nanoparticles during the XPS sampling procedure is a well known phenomenon.[44,45] FT-RAMAN spectral analysis was performed to ensure the presence of NiO on the surface of the catalyst since FT-RAMAN is a very useful technique to detect metal oxide. The RAMAN spectra of  $\text{Fe}_3\text{O}_4$  and  $\text{Fe}_3\text{O}_4@\text{AHBA}@\text{Ni}(0)$  resemble closely. Thus it can be concluded that NiO nanoparticles formed during XPS study as impurity.

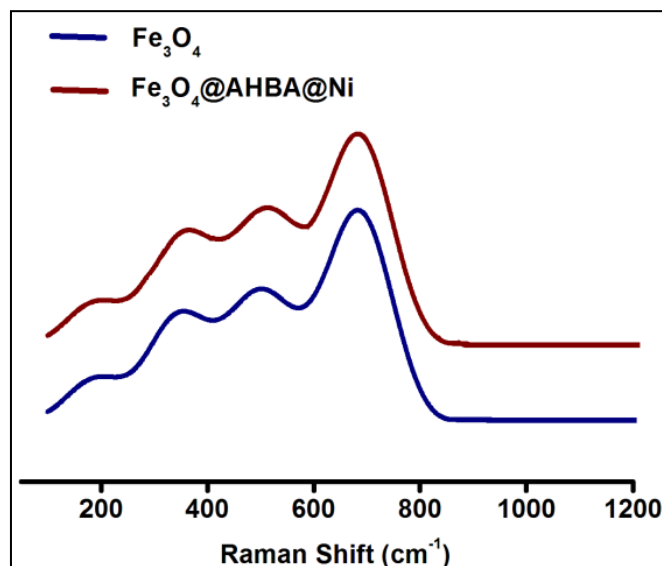


**Fig. 3.** FT-RAMN spectrum of  $\text{Fe}_3\text{O}_4$  and  $\text{Fe}_3\text{O}_4@\text{AHBA}@\text{Ni}(0)$  catalyst

The presence of Ni(0) on the surface of  $\text{Fe}_3\text{O}_4@\text{AHBA}@\text{Ni}(0)$  was further confirmed by time of flight secondary ion mass spectrometry (TOF-SIMS), a commonly used technique for surface characterization. The spectra of catalyst in positive ion mode consist of two peak at  $m/z=58$  and  $60$  due to two most abundant isotopes of Nickel which suggest the presence of Ni at the surface of it. The peak at  $m/z=56$  arises for  $^{56}\text{Fe}^+$ , present in the  $\text{Fe}_3\text{O}_4$  moiety. In the range of  $m/z = 60$  to  $100$  an additional peak at  $m/z=61, 62, 69$  and  $73$  appears due to  $^{61}\text{Ni}^+, ^{62}\text{Ni}^+, \text{FeO}$  and  $\text{FeOH}^+$  respectively (Fig. 4).

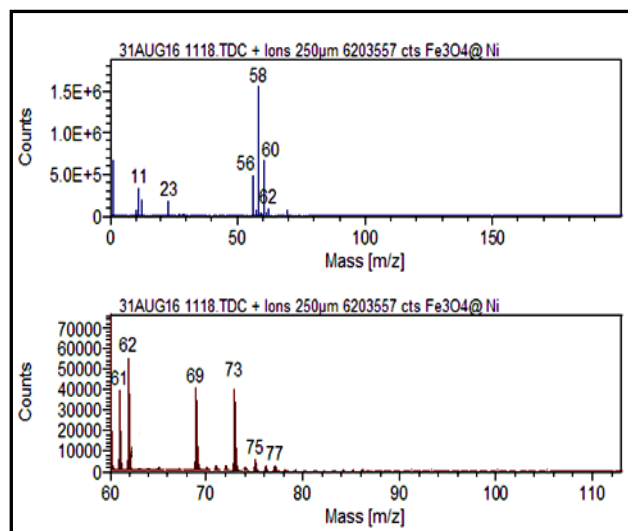


**Fig. 4.** TOF-SIMS positive ion spectra of  $\text{Fe}_3\text{O}_4@AHBA@Ni(0)$  catalyst

The degree of crystalline nature of magnetic  $\text{Fe}_3\text{O}_4$  and  $\text{Fe}_3\text{O}_4@AHBA@Ni(0)$  were verified from Power X-Ray Diffraction (PXRD) measurements (Fig. S4). The PXRD data fit well with the standard  $\text{Fe}_3\text{O}_4$  sample. The same peaks were observed among the  $\text{Fe}_3\text{O}_4@AHBA@Ni(0)$  in PXRD patterns, signifying that the grafting process does not induce any phase change of  $\text{Fe}_3\text{O}_4$  as we observed earlier.[14, 33-34] Scanning electron microscopy (SEM) image of  $\text{Fe}_3\text{O}_4@AHBA@Ni(0)$  was quite different from those of our prepared  $\text{Fe}_3\text{O}_4$ -NPs. [14, 33-34]

The SEM images of nanocatalyst contained agglomerated particle and this alteration in morphology confirms the surface modification process (Fig. 5). A close verification of transmission electron microscopy (TEM) image of  $\text{Fe}_3\text{O}_4@AHBA@Ni(0)$  revealed that these magnetic nanoparticles are spherical with an average diameter of  $10.0853 \pm 4.36$  nm (Fig. 6a). From the histogram of TEM image it is observed that most abundant average diameter of nanoparticles is 10.085 nm (Fig. 6b).

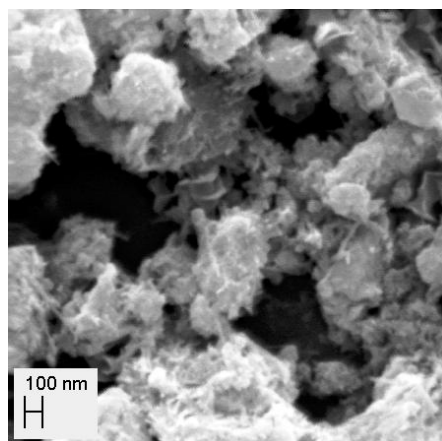


**Fig. 5.** SEM images of  $\text{Fe}_3\text{O}_4@AHBA@Ni(0)$

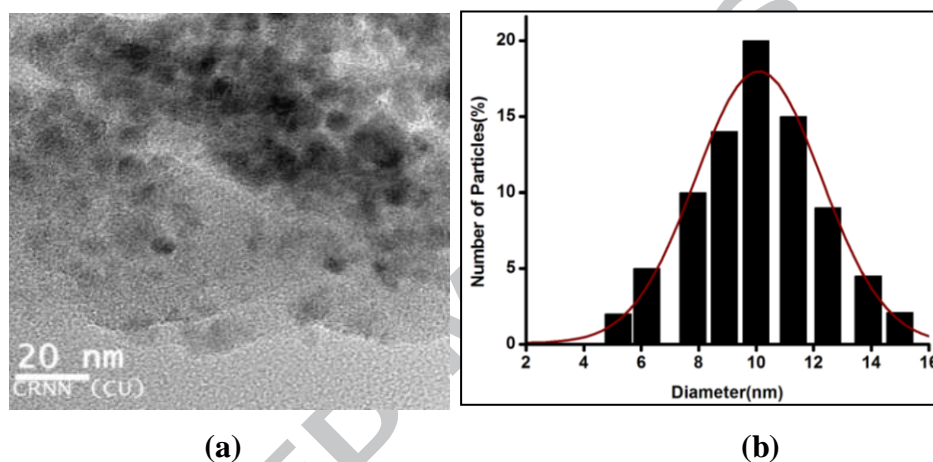


**Fig. 6.** (a) TEM images and (b) histogram of  $\text{Fe}_3\text{O}_4@AHBA@Ni(0)$

The Energy-dispersive X-ray (EDX) spectra of  $\text{Fe}_3\text{O}_4@AHBA@Ni(0)$  nanocatalyst are depicted in (Fig. S5). The well-defined peaks of nickel in the EDX spectrum of nanocatalyst confirm its presence in nanocatalyst. Magnetization behaviour of  $\text{Fe}_3\text{O}_4$  NPs and  $\text{Fe}_3\text{O}_4@AHBA@Ni(0)$  was studied under applied magnetic field and is shown in Fig. 7. The curves exhibit very similar phenomenon as we have observed earlier. [14, 33-34] The decrease in the values of the saturation magnetization ( $M_s$ ) from the  $\text{Fe}_3\text{O}_4$  nanoparticles ( $62.5 \text{ emu g}^{-1}$ ) to  $\text{Fe}_3\text{O}_4@AHBA@Ni$  ( $35.1 \text{ emu g}^{-1}$ ) due to gradual increment of organic moiety from  $\text{Fe}_3\text{O}_4$  NPs to  $\text{Fe}_3\text{O}_4@AHBA@Ni$ . However, the net magnetism showed by the final nanocatalyst is satisfactorily good for an effective separation from the solution medium through the use of an external magnetic force.

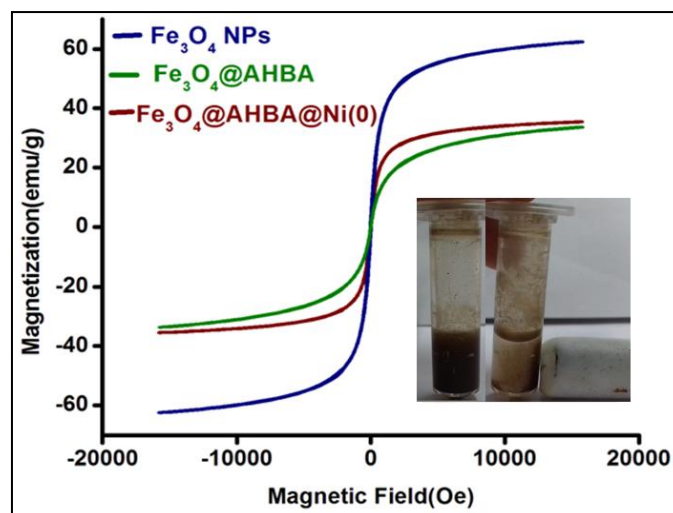
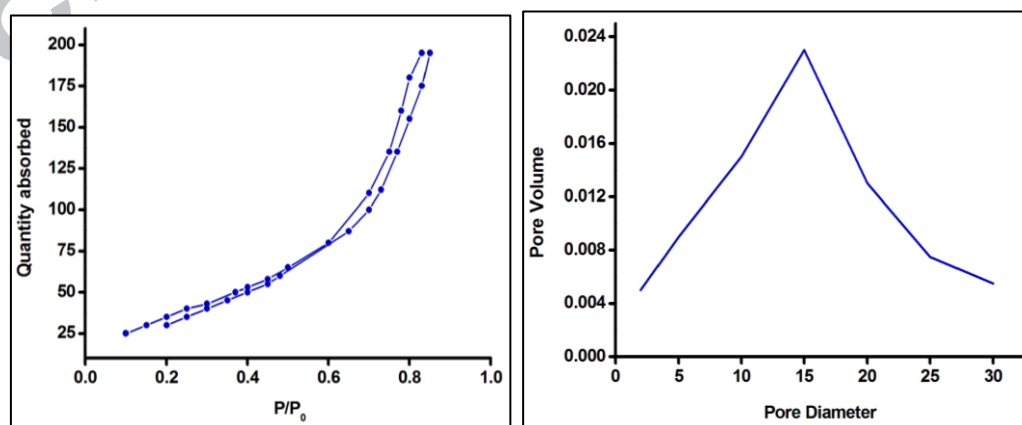


**Fig. 7.** Magnetic curves of  $\text{Fe}_3\text{O}_4$ ,  $\text{Fe}_3\text{O}_4@AHBA$  and  $\text{Fe}_3\text{O}_4@AHBA@Ni(0)$

The measurement of the hydrodynamic size of  $\text{Fe}_3\text{O}_4@AHBA@Ni$  nanocatalyst by dynamic light scattering (DLS) shows stable non-aggregated particles with a mean diameter of 40 nm (Fig. S6). They show good stability in water.

The textural properties of the  $\text{Fe}_3\text{O}_4@AHBA@Ni(0)$  nanocatalyst was investigated by Brunauer-Emmett-Teller (BET) gas-sorption measurements carried out at 77 K for the as-dried powder sample under vacuum, as shown in (Fig. 8). BET surface area of  $\text{Fe}_3\text{O}_4@AHBA@Ni(0)$  nanocatalyst was  $330 \text{ m}^2 \text{ g}^{-1}$ , very similar close to earlier report. The nitrogen adsorption isotherm holds a sharp inflection point at  $P/P_0 = 0.55$ . The pore size distribution adsorption curve is situated at 15.0 nm. It is evident that our synthesized nanocatalyst has high BET surface areas which provide a platform for the catalytic organic transformation.



(a)

(b)

**Fig. 8.** (a) Nitrogen sorption isotherm and (b) BJH pore size distribution of the  $\text{Fe}_3\text{O}_4@\text{AHBA}@\text{Ni}(0)$

3.2. *Reduction of carbonyl catalyzed by  $\text{Fe}_3\text{O}_4@\text{AHBA}@\text{Ni}(0)$ .* In order to explore the efficacy of the catalyst towards organic reaction, reduction of carbonyls were carried out using glycerol as hydrogen source as well as solvent. All the carbonyl compounds mentioned in Table 1 were successfully reduced to their corresponding alcohols. In this study, optimization of the reaction conditions for carbonyls reduction was also carried out, making an allowance for substrate (benzaldehyde)/ reductant(glycerol) molar ratio and the duration of reaction time . It was observed that the conversion remains constant after 3 h of reaction. The effect of the concentration of the catalyst with respect to the model substrate was also studied. In absence of catalyst the conversion was significantly low (Table S1, entry 1). The maximum conversion is observed when the reduction was performed in presence of 30 mg of catalyst and 3 ml of glycerol (Table 1, entry 5). Interestingly, the conversion decreased with an increased amount of catalyst (Table 1, entry 8) in case of reduction of carbonyl. This is probably due to a decrease in the surface area of the nanocatalyst caused by adsorption of reduced or oxidized products on the active surface. Further, the reduction reactions were extended to a variety of carbonyls using the optimized reaction conditions as tabulated in Table 2. Here we thought similar mechanistic path as reported in literature. [46]

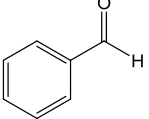
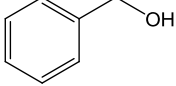
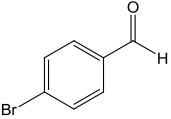
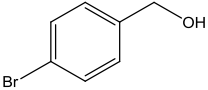
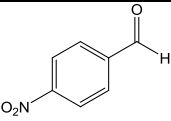
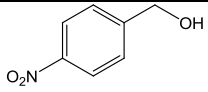
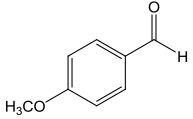
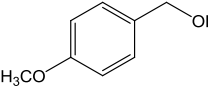
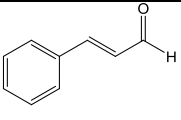
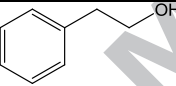
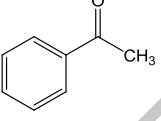
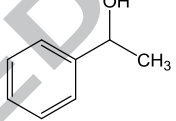
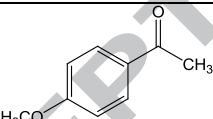
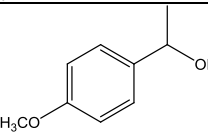
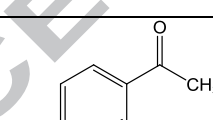
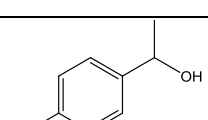
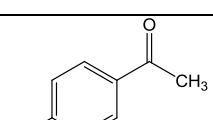
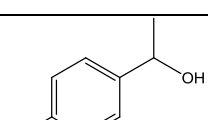
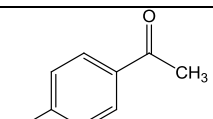
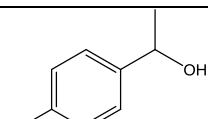
**Table 1.**

Optimization of reaction conditions for reduction of benzaldehyde

Entry	Catalyst(mg)	Amount of reductant (mL)	Conversion <sup>a</sup> (%)
1	0	3.0	<1
2	5	3.0	17
3	10	3.0	38
4	20	3.0	74
<b>5</b>	<b>30</b>	<b>3.0</b>	<b>90</b>
6	30	2.5	85
7	30	3.5	<b>82</b>
8	35	3.0	16

<sup>a</sup> Reaction conditions: substrate 1 mmol, time(3 h)

**Table 2** $\text{Fe}_3\text{O}_4@\text{AHBA}@\text{Ni}(0)$  catalyzed reduction of carbonyls <sup>a</sup>

Entry	Compound	Product	Time (h)	Conversion (%)	Yield (%)
1			3	93	90
2			3	89	87
3			3	91	89
4			3	92	88
5			3	94	92
6			3	95	90
7			3	89	87
8			3	93	88
9			3	88	85
10			3	87	83

<sup>a</sup> Reaction conditions: substrate 1 mmol, KOH 2 mmol,  $\text{Fe}_3\text{O}_4@\text{AHBA}@\text{Ni}(0)$  30 mg, glycerol 3 mL.

### 3.3. Oxidation of alcohol catalyzed by $Fe_3O_4@AHBA@Ni(0)$ .

Herein we report a novel protocol that employs  $Fe_3O_4$  supported Ni(0)-nanoparticles as an efficient catalyst for oxidation of alcohols. Here we have chosen iodobenzene diacetate [ $PhI(OAc)_2$ ] as reagents oxidation, due to its unique properties.[47] The results for the oxidation of a variety of alcohols are summarized in Table 4. In this case optimization of the reaction conditions for alcohols oxidation by the nanocatalyst was also monitored, taking into account the influence of substrate (benzyl alcohol)/oxidant molar ratio and duration of the reaction time (Table 3). It was observed that the conversion remains constant after a reaction time of 3 h. The effect of the concentration of the catalyst with respect to the model substrate was studied. A significant conversion with 20 mg of the catalyst was observed for alcohol oxidation respectively (Table 3, entry 5). The conversion observed in the absence of the catalyst was very low (Table 3, entry 1). This revealed the catalytic role of our synthesized  $Fe_3O_4@AHBA@Ni(0)$ . The conversion decreased with an increased amount of catalyst (Table 3, entry 8) also in case of oxidation of alcohol. This is probably due to a decrease in the surface area of the nanocatalyst caused by adsorption of reduced or oxidized products on the active surface. The oxidation reactions were extended to a variety of alcohols using the optimized reaction conditions (Table 4).

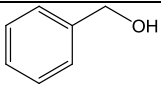
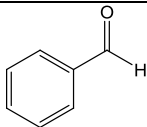
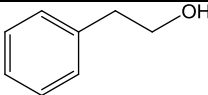
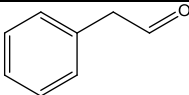
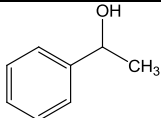
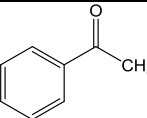
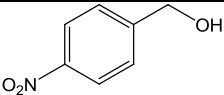
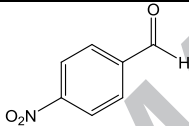
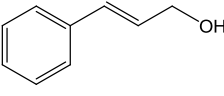
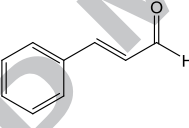
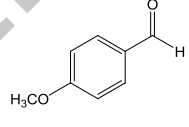
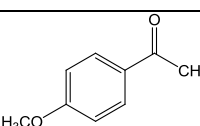
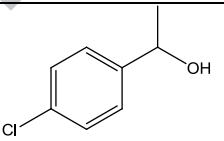
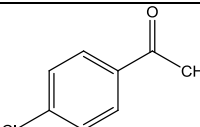
**Table 3**

Optimization of reaction conditions for oxidation of benzyl alcohol

Entry	Catalyst(mg)	Amount of oxidant (mmol)	Conversion <sup>a</sup> (%)
1	0	1.25	<1
2	5	1.25	21
3	10	1.25	48
4	15	1.25	77
<b>5</b>	<b>20</b>	<b>1.25</b>	<b>92</b>
6	20	1.00	88
7	20	1.50	84
8	25	1.25	18

<sup>a</sup> Reaction conditions: substrate 1 mmol, ethylenedichloride 25 mL, time(3 h)

**Table 4**Fe<sub>3</sub>O<sub>4</sub>@AHBA@Ni(0) catalyzed oxidation of alcohols <sup>a</sup>

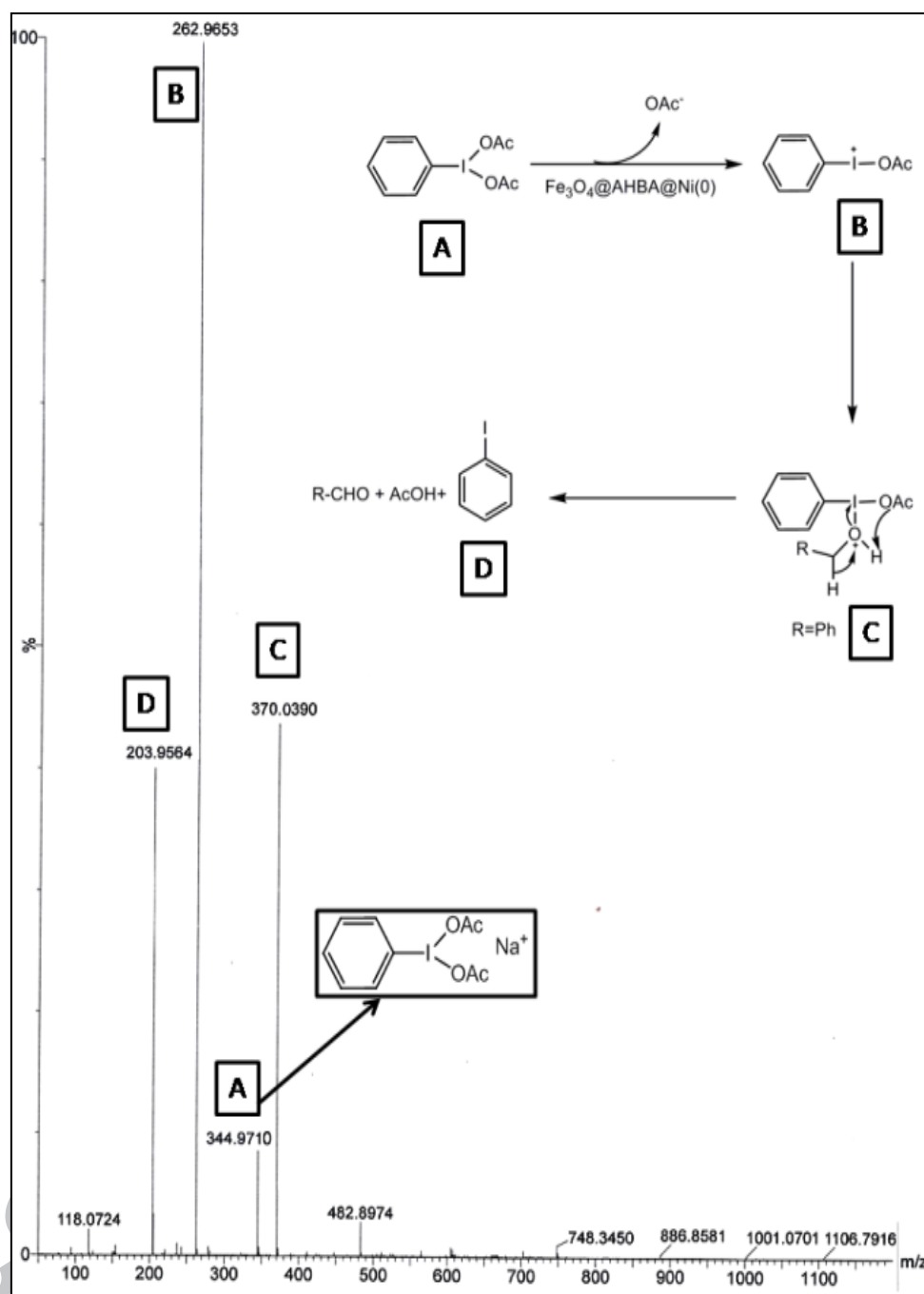
Entry	Compound	Product	Time (h)	Conversion (%)	Yield (%)
1			3	83	92
2			3	80	90
3			3	75	82
4			3	80	86
5			3	79	87
6			3	75	80
7			3	76	80
8			3	78	82

<sup>a</sup> Reaction conditions: substrate 1 mmol, PhI(OAc)<sub>2</sub> (1.25 mmol), Fe<sub>3</sub>O<sub>4</sub>@AHBA@Ni(0) 20 mg, ethylenedichloride 25 mL.

### 3.4. Probable mechanistic pathway for oxidation of alcohol.

In order to establish a plausible mechanism for the oxidation of alcohol ESI-MS study of reaction mixture was carried out after 1 hour of the reaction. The reaction was performed using benzyl alcohol as substrate. The intermediates are characterized by the ESI-MS study after careful separation of the catalyst from reaction mixture. Firstly, the catalyst ruptured one

of the I-OAc bond of  $[\text{PhI}(\text{OAc})_2]$  to generate  $\text{OAc}^-$  and  $[\text{PhI}(\text{OAc})]^+$  ions.  $[\text{PhI}(\text{OAc})]^+$  ion plays an important role for oxidation of the substrates. Peaks at  $m/z = 262.9653$  amu for  $[\text{PhI}(\text{OAc})]^+$  ion and  $344.9710$  amu for  $[\text{PhI}(\text{OAc})_2]\text{-Na}^+$  are observed along with the peak at  $370.0390$  amu assigned to  $[\text{PhI}(\text{OAc})]^+\text{-PhCH}_2\text{OH}$  adduct as reported earlier.[48] The proposed mechanism for alcohol oxidation with  $[\text{PhI}(\text{OAc})_2]$  as oxidant is represented in Scheme 2. The unreduced  $\text{Fe}_3\text{O}_4\text{@AHBA@Ni(II)}$  can oxidized alcohol but  $\text{OAc}^-$  ion which was generated during the catalytic reaction leached Ni(II) from  $\text{Fe}_3\text{O}_4\text{@AHBA@Ni(II)}$  and deactivated its catalytic property (Fig. S7). Thus we reduced Ni(II) to Ni(0) to overcome this problem.



**Scheme 2.**ESI-MS study of reaction solution of oxidation of alcohol

3.5. *Reusability of Fe<sub>3</sub>O<sub>4</sub>@AHBA@Ni(0)*. Application of a simple bar magnet at the end of the reaction ensures the separation of our synthesized nanocatalyst. This was washed with acetone, dried at 60°C which can be reused further for seven times (Fig. 9) without significant loss of catalytic activity in the model reactions.

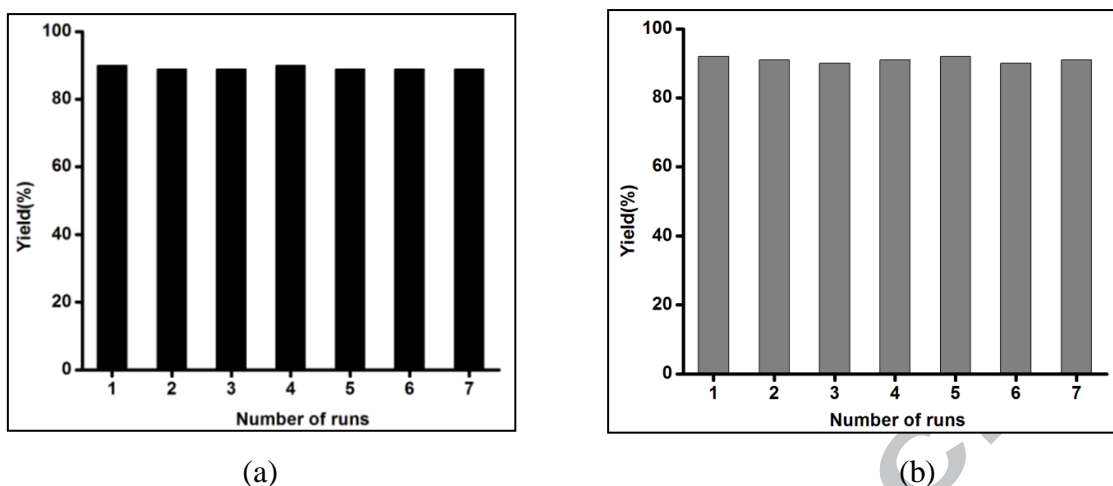


**Fig. 9.** Reusability of Fe<sub>3</sub>O<sub>4</sub>@AHBA@Ni(0) towards: (a) reduction of benzaldehyde and (b) oxidation of benzyl alcohol

The used catalyst has been further characterized by SEM after second, fourth and seventh cycle in case of both oxidation and reduction (Fig. S8,S9) and TEM (Fig. S10). The size, shape and morphology of the nanoparticles is same as was before the reaction, which clearly indicates that no structural deformation takes place in catalyst active site. This was the possible key factor for its reusability.

#### 4. Conclusions

In summary, we have developed an economically viable and energy efficient catalytic a new method using nickel based nanocatalyst for the reduction of carbonyls and oxidation of alcohols in ambient condition at room temperature. Our synthesized catalyst showed excellent catalytic properties towards oxidation as well as reduction (Yield  $\geq$  80%) reactions. Here, we have also demonstrated that nickel in its zero oxidation state which can play a very interesting role and also established a new mechanistic path for oxidation of alcohol. The simple process, stability of catalyst, use of economical and gentle magnetic nanoparticles as support, effortless recoverability and reusability, and above all, the yield in short reaction time with little effluent discharge makes it an environmentally acceptable and greener alternative, when compared to the other reported method. The recyclability test confirmed that the catalyst could be reused at least seven times without any major degradation in its activity. We speculate that this novel catalytic system would find functions in several other industrially important catalytic processes as well as the common synthetic organic transformations.

## Acknowledgements

Financial support by the Science and Engineering Research Board (a statutory body under DST, New Delhi, India (F. No. SB/FT/CS-185/2013 dt. 30-06-2014) is gratefully acknowledged by TC. SD is thankful to UGC and University of Calcutta [UGC/485/Fellow (univ)] for providing fellowship.

## References

- [1] M. Turner, V. B. Golovko, O. P. H. Vaughan, P. Abdulkin, A. Berenguer-Murcia, M. S. Tikhov, B. F. G. Johnson, R. M. Lambert, *Nature*. 454 (2008) 981.
- [2] Z. Chen, Z. Jiao, D. Pan, Z. Li, M. Wu, C-H. Shek, C. M. L. Wu, K. L. L. Joseph, *Chem. Rev.* 112 (2012) 3833.
- [3] W. Weifeng, C. Xinwei, C. Weixing, G. I. Douglas, *Chem. Soc. Rev.* 40 (2011) 1697.
- [4] G. S. Thomas, J. R. Bargar, S. Garrison, M. T. Bradley, *Acc. Chem. Res.* 43 (2010) 2.
- [5] C. N. R. Rao, A. Muller, A. K. Cheetham, *The Chemistry of Nanomaterials: Synthesis and Applications*, Vol. 1, Wiley-VCH, Weinheim 2004, pp.555.
- [6] B. M. Choudary, S. Madhi, N. S. Chowdari, M. L. Kantam, B. Sreedhar, *J. Am. Chem. Soc.* 124 (2002) 14127.
- [7] L. Djakovitch, K. Koehler, *J. Am. Chem. Soc.* 123 (2001) 5990.
- [8] B. P. Chauhan, J. S. Rathore, M. Chauhan, A. Krawicz, *J. Am. Chem. Soc.* 125 (2003) 2876.
- [9] M. Ooe, M. Murata, T. Mizugaki, K. Ebitani, K. Kaneda, *J. Am. Chem. Soc.* 126 (2004) 1604.
- [10] S. Kidambi, J. Dai, J. Li, M. L. Bruening, *J. Am. Chem. Soc.* 126 (2004) 2658.
- [11] J. Huang, T. Jiang, H. Gao, B. Han, Z. Liu, W. Wu, Y. Chang, G. Zhao, *Angew. Chem. Int. Ed.* 43 (2004) 1397.
- [12] J. Dupont, G. S. Fonseca, A. P. Umpierre, P. F. P. Fichtner, S. R. Teixeira, *J. Am. Chem. Soc.* 124(2002) 4228.
- [13] M. Beller, H. Fisher, K. Kuhlein, C.P. Reisinger, W.A. Herrmann, *J. Organomet. Chem.* 520(1996) 257.
- [14] J. Adhikary, A. Datta, S. Dasgupta, A. Chakraborty, M.I. Menéndez, T. Chattopadhyay, *RSC Adv.* 5(2015)92634.

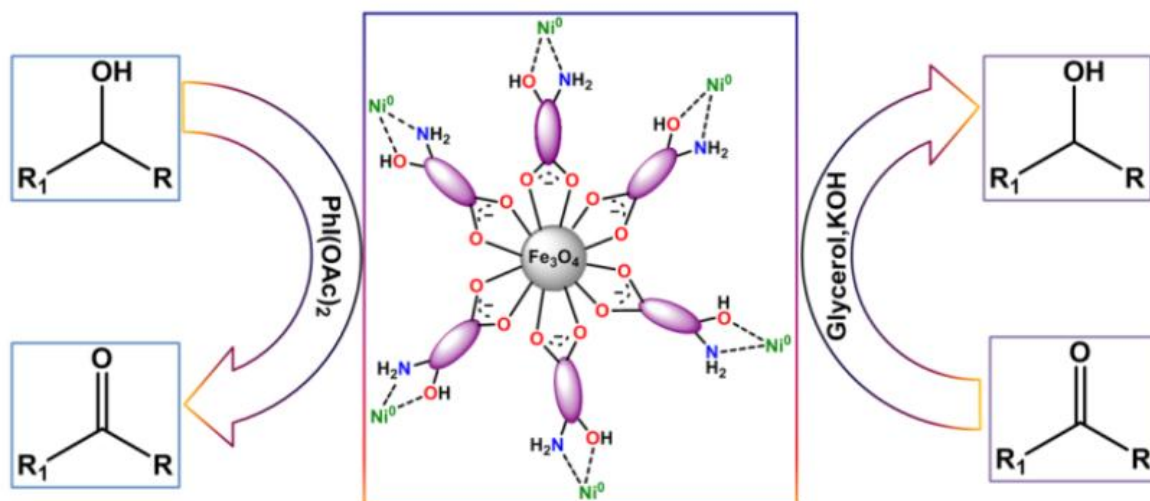
- [15] H. Meyer, F. Winkler, P. Kunz, A.M. Schmidt, A. Hamacher, M.U. Kassack, C. Janiak, *Inorg. Chem.* 54(2015)11236.
- [16] M. Shokouhimehr, Y. Piao, J. Kim, Y. Jang, T. Hyeon, *Angew. Chem. Int. Ed.* 46(2007)7039.
- [17] M.B. Gawande, P.S. Branco, R.S. Varma, *Chem. Soc. Rev.* 42 (2013) 3371.
- [18] R.B.N. Baig, M.N. Nadagouda, R.S. Varma, *Coord. Chem. Rev.* 287 (2015) 137.
- [19] S. Xuan, Y-X. J. Wang, J. C. Yu, K. C-F. Leung, *Langmuir.* 25(2009)11835.
- [20] A. Silvestri, S. Mondini, M. Marelli, V. Pifferi, L. Falciola, A. Ponti, A. M. Ferretti, L. Polito, DOI: 10.1021/acs.langmuir.6b01266.
- [21] L. Zhou , C. Gao , W. Xu, *Langmuir* . 26(2010)11217.
- [22] M. Li, X. Li, X. Qi, F. Luo, G. He, DOI: 10.1021/acs.langmuir.5b00800.
- [23] N. Yan, C. Xiao, Y. Kou, *Coord. Chem. Rev.* 254(2010) 1179
- [24] V. Polshettiwar, R. Luque, A. Fihri, H. Zhu, M. Bouhrara, J-M Basset, *Chem. Rev.* 111(2011) 3036.
- [25] S . Z. Tasker<sup>1</sup>, E. A. Standley, T. F. Jamison, *Nature.* 509(2014)299.
- [26] B.Cordero, V. Gomez, A. E. Platero-Prats, M.Reves, J.Echeverria, E.Cremades, F. Barragan, S .Alvarez. *Dalton Trans.* (2008) 2832.
- [27] B. M. Choudary, M. L. Kantam, A. Rahman, C. V. Reddy, K. K. Rao, *Angew. Chem., Int. Ed.* 40(2001)763 .
- [28] S. K. Mohapatra, S. U.Sonavane, R. V. Jayaram, P. Selvam, *Org. Lett.* 4(2002) 4297.
- [29] B. M.Choudary, M. L. Kantam, A. Rahman, C. V. Reddy, *J. Mol. Catal. A: Chem.* 206 (2003) 145.
- [30] T. Chattopadhyay, M. Kogiso, M. Aoyagi, H. Yui, M. Asakawa, T. Shimizu, *Green Chem.* 13(2011)1138.
- [31] P. B. Bhat, B. R. Bhat, *New J. Chem.* 39(2015)273.
- [32] P. B. Bhat, F. Inam, B. R. Bhat, *ACS Comb. Sci.* 16(2014) 397.
- [33] A. Datta, J. Adhikary, S. Chatterjee, D. Ghosh, S. Khamarui, T. Chattopadhyay; *Inorg. Chim. Acta* . 444(2016) 209.
- [34] T. Chattopadhyay, A. Chakraborty, S. Dasgupta, A. Dutta, M. I. Menéndez, E. Zangrando, *Appl Organometal Chem*, DOI :10.1002/aoc.3663.
- [35] R. P. Singh, R. Patidar, T. Shripathic, S. Thakore, *Catal. Sci. Technol.* 5 (2015)286.
- [36] E. Karaoglu, A. Baykal, M. Şenel, H. Sözeri, M. S. Toprak, *Materials Research Bulletin.* 47 (2012) 2480.
- [37] V. Polshettiwar, B. Baruwati , R. S. Varma, *Green Chem* .11( 2009)127.

- [38] J. Adhikary, P. Chakraborty, B. Das, A. Datta, S. K. Dash, S. Roy, J-W Chen, T. Chattopadhyay, *RSC Adv.* 5(2015) 35917.
- [39] D. Özhava, N. Z. Kılıcaslan, S. Özkar, *Applied Catalysis B: Environmental* 162 (2015) 573.
- [40] G. Ertl, R. Hierl, H. Knozinger, N. Thiele, H.P. Urbach, *Appl. Surf. Sci.* 5 (1980)49.
- [41] A.N. Mansour, *Surf. Sci. Spectra* 3 (1994) 211.
- [42] S.O. Grim, L.J. Matienzo, W.E. Swartz, *J. Am. Chem. Soc.* 94 (1972) 5116.
- [43] A. N. Mansour, *Surf. Sci. Spectra* 3 (1994) 231.
- [44] M.Zahmakıran1, T.Ayvalı, S. Akbayrak, S. Calıskan, D.Celik, S. Ozkar, *Catalysis Today* 170 (2011) 76.
- [45] L. Gucci, D. Bazin, *Appl. Catal. A: Gen.* 188 (1999) 163-174.
- [46] A. E. Díaz-Álvarez, V. Cadierno, *Applied Sciences* 3(2013) 55.
- [47] H. Nishiyama, T. Shimada, H. Itoh, H. Sugiyama, Y. Motoyama, *Chem. Commun.* (1997) 1863.
- [48] Y-B. Kang, L. H. Gade, *J. Am. Chem. Soc.* 133(2011) 3658.

**Highlights**

A magnetically separable Ni(0) nanocatalyst has been prepared and explored for its dual catalytic activity.

ACCEPTED MANUSCRIPT



ACCEPTED MANUSCRIPT